

From Precursors to Ceramic Materials.

II. Synthesis and Specific Features of New Garnet Structure Compounds

I. Pakutinskiene^{1,2}, S. Mathur³, H. Shen³, G. Kudabiene², D. Jasaitis¹, A. Kareiva^{1*}

¹Department of General and Inorganic Chemistry, Vilnius University, Naugarduko 24, LT-2006 Vilnius, Lithuania

²Department of Chemistry, Vilnius Pedagogical University, Studentų 39, LT-2034 Vilnius, Lithuania

³Institute of New Materials, University of Saarland, D-66123, Saarbruecken, Germany

Received 16 September 2003; accepted 21 October 2003

In this paper, the sol-gel synthesis and characteristic properties of mixed-metal oxides $Y_3Sc_xAl_{5-x-y}Ga_yO_{12}$ ($0 \leq x, y \leq 5$) having garnet crystal structure are reported. The polycrystalline powders were characterized by powder X-ray diffraction analysis (XRD), energy dispersive X-ray (EDX) analysis, IR spectroscopy and optical transmission measurements. Single-phase oxides $Y_3Sc_1Al_3Ga_1O_{12}$, $Y_3Sc_2Al_1Ga_2O_{12}$, $Y_3Sc_2Al_3O_{12}$ and $Y_3Al_3Ga_2O_{12}$ have been synthesized at 1000 °C. The transmittance spectra of $Y_3Sc_xAl_{5-x-y}Ga_yO_{12}$ samples were measured at room temperature in the range of 200 – 1200 nm.

Keywords: YSAGG, mixed-metal garnets, substitution effects, optical materials.

INTRODUCTION

The use of aluminum compounds for electronic and optical applications shows an increased activity during past years. An important feature of metallic aluminum is the fact it auto-oxidizes to form a corrosion-resistant surface coating of alumina. Alumina is an unreactive thermally stable ceramics. There are several common forms of this material, each with its own set of unique applications [1]. Although the applications of aluminum oxides themselves are extensive, ternary systems, such as mullite, garnet, hibonite and β -alumina can offer advantages over those of the binary aluminum oxides [2 – 6].

The overall objective of the part of our research project is to search for advanced optical materials starting from low cost, air stable gel preceramic precursor [7 – 9]. To achieve this goal, recently the sol-gel method based on metal chelates in aqueous solvents has been developed to prepare pure and rare-earth doped yttrium aluminum garnet (YAG) [10, 11]. Moreover, the same sol-gel technique has been used for the synthesis of multimetallic oxides $Y_3Sc_xAl_{5-x-y}Ga_yO_{12}$ ($0 \leq x, y \leq 5$) (YSAGG), having complicated both chemical composition and garnet crystal structure [12 – 14]. We have demonstrated, that the sol-gel methods based on molecular precursors have a cutting edge over the other solution routes because they allow chemical interactions among the initial mixture of precursor species favoring the evolution of solid-state structure at the atomic level [15, 16].

The aim of this study was the evaluation of some specific features of different sol-gel derived mixed-metal garnets $Y_3Sc_xAl_{5-x-y}Ga_yO_{12}$. The paper describes the results concerning the synthesis, phase transformations, composition and optical properties of YSAGG compounds.

EXPERIMENTAL

Six samples $Y_3Sc_xAl_{5-x-y}Ga_yO_{12}$ ($0 \leq x, y \leq 5$) with different nominal composition, $Y_3Al_5O_{12}$ (YAG),

$Y_3Sc_2Al_1Ga_2O_{12}$ (YSAGG–212), $Y_3Sc_1Al_3Ga_1O_{12}$ (YSAGG–131), $Y_3Sc_2Al_3O_{12}$ (YSAG), $Y_3Al_3Ga_2O_{12}$ (YAGG), $Y_3Sc_{2.5}Ga_{2.5}O_{12}$ (YSGG) were synthesized by aqueous sol-gel method. The gels were prepared according to the previously reported methodology [12]. The oven dried (110 °C) gel powders were ground in an agate mortar and preheated for 2 h at 800 °C in air. After an intermediate grinding in an agate mortar the powders were additionally sintered for 10 h at 1000 °C in air.

The synthesized samples were characterized by X-ray powder analysis (XRD) performed with a Siemens D-5000 powder diffractometer using $CuK\alpha_1$ radiation. The energy dispersive X-ray (EDX) analysis was performed, in vacuum, in the specimen chamber of an EDX coupled scanning electron microscope (SEM) CAM SCAN S4. The infrared (IR) spectra were recorded as KBr pellets on a BioRad FTIR–165 spectrometer. The optical transmission measurements of the garnet samples were carried out using SF-26 spectrophotometer at room temperature with a fused-quartz glass substrate inserted into the reference beam path of the spectrophotometer.

RESULTS AND DISCUSSION

The X-ray diffraction patterns for the calcined precursor gel powders and sintered for 10 h at 1000 °C are shown in Fig. 1. As seen, the samples fully crystallize, and the obtained phases slightly depend on the nominal composition of precursor gels. According to XRD analysis, sintering precursor gels at 1000 °C produced fully crystalline single-phase oxides $Y_3Sc_1Al_3Ga_1O_{12}$, $Y_3Sc_2Al_1Ga_2O_{12}$, $Y_3Sc_2Al_3O_{12}$ and $Y_3Al_3Ga_2O_{12}$, which have well pronounced garnet crystal structure [7, 8, 10, 17, 18]. However, it is clear from Fig. 1 that the formation of $Y_3Sc_{2.5}Ga_{2.5}O_{12}$ garnet does not proceed under similar experimental conditions.

It is well known that in a crystalline garnet structure the cations are distributed among tetrahedral, octahedral and dodecahedral interstices [19]. The cations possibly may redistribute themselves, subject to the size of the individual ions, in order to stabilize the crystalline

*Corresponding author. Tel.: + 370-5-2336214; fax: + 370-5-2330987.
E-mail address: aivaras.kareiva@chf.vu.lt (A. Kareiva)

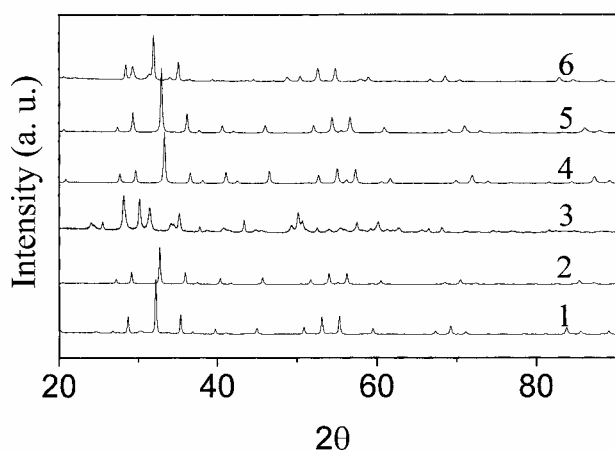


Fig. 1. X-ray diffraction patterns of the $Y_3Sc_xAl_{5-x-y}Ga_yO_{12}$ ceramic samples synthesized at 1000 °C: (1) YAG, (2) YSAGG-212, (3) YSGG, (4) YSAG, (5) YAGG and (6) YSAGG-131

structure. We propose that such cationic distribution and the stabilization are related to a critical value of octahedral and dodecahedral radii (Al sites) where the substitution takes place. The cationic radii for the different compositions are listed in Table 1.

Table 1. The mean cationic radii at Al sites for the different $Y_3Sc_xAl_{5-x-y}Ga_yO_{12}$ compositions

Garnet sample	Mean cationic radius (Å)
$Y_3Al_5O_{12}$ (YAG)	0.390
$Y_3Al_3Ga_2O_{12}$ (YAGG)	0.422
$Y_3Sc_1Al_3Ga_1O_{12}$ (YSAGG-131)	0.478
$Y_3Sc_2Al_3O_{12}$ (YSAG)	0.534
$Y_3Sc_2Al_1Ga_2O_{12}$ (YSAGG-212)	0.566
$Y_3Sc_{2.5}Ga_{2.5}O_{12}$ (YSGG)	0.610

In view of the above, possible interpretation for the instability of the $Y_3Sc_{2.5}Ga_{2.5}O_{12}$ phase is that at this molar ratio the mean cationic radius of the composition (0.610 Angstroms) exceeds this critical value. The mean cationic radii for the phases forming a stable garnet structure are lower than the value observed for $Y_3Sc_{2.5}Ga_{2.5}O_{12}$. This shows that the further substitution of smaller Ga ions (0.47 Angstroms) through much larger Sc ions (0.75 Angstroms) causes the destabilization of the garnet structure. However, from the above discussions it is apparent that a systematic study of the small structural changes induced by Ga and Sc substitution in YAG should be performed.

Evidently, these XRD diffraction patterns show some negligible shift in the position of diffraction lines. This feature probably is caused by different unit size of garnet samples with different composition. It is well known that unit size is very much affected by variation of lattice parameters for substituted mixed-metal oxides [20, 21]. For the single-phase $Y_3Sc_xAl_{5-x-y}Ga_yO_{12}$ samples the most intensive (100 %) lines from the plane having Miller indices (420) are located in the range of $2\theta = 32.0 - 33.5^\circ$ (see Fig. 1). It is known, that Bragg's law treats X-rays as being diffracted from various sets of lattice planes and the

Bragg diffraction angle, θ , for each set is related to the d -spacing by Bragg's law [22]. Fig. 2 shows the dependence of the calculated d -spacing of a set of (420) planes on the mean cationic radii at Al sites for the single-phase $Y_3Sc_xAl_{5-x-y}Ga_yO_{12}$ ceramic samples.

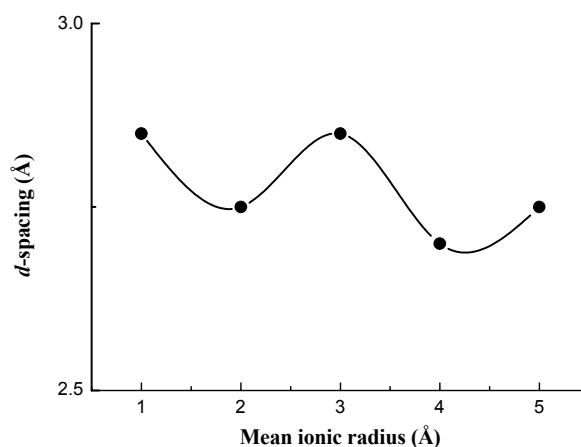


Fig. 2. Relationship between d -spacing of (420) and mean cationic radius of the $Y_3Sc_xAl_{5-x-y}Ga_yO_{12}$ samples

The random distribution of the results is seen indicating that no linear correlation between d -spacing and the mean cationic radius of the $Y_3Sc_xAl_{5-x-y}Ga_yO_{12}$ samples could be observed.

EDX analyses were also carried out on the single-phase $Y_3Sc_xAl_{5-x-y}Ga_yO_{12}$ samples. The EDX spectrum for $Y_3Al_5O_{12}$ sample is shown presented in Fig. 3.

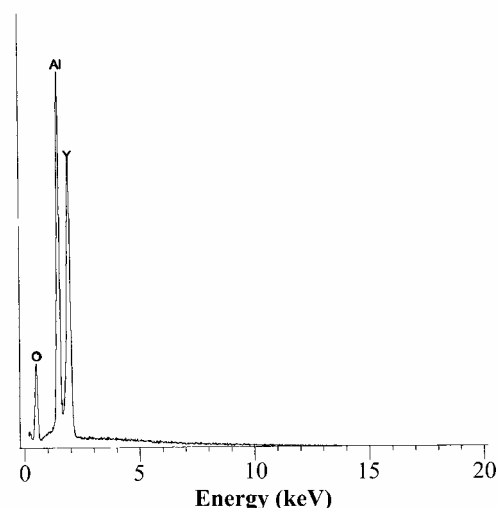


Fig. 3. Energy dispersive X-ray spectrum of $Y_3Al_5O_{12}$ ceramic sample

From Fig. 3 is evident that only yttrium, aluminium and oxygen are present in the sample, and no other elements can be detected from the EDX spectrum. These results confirm that synthesized YAG sample is of high purity and good quality. The EDX spectra of two representative YSAGG ceramic samples ($Y_3Sc_2Al_1Ga_2O_{12}$ and $Y_3Sc_1Al_3Ga_1O_{12}$) are presented in Figs. 4 and 5, respectively.

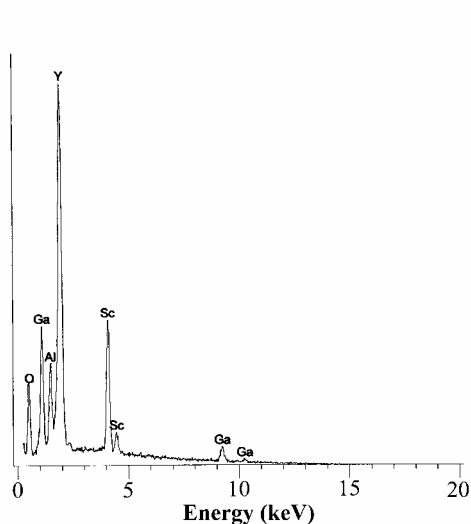


Fig. 4. Energy dispersive X-ray spectrum of $Y_3Sc_2Al_1Ga_2O_{12}$ ceramic sample

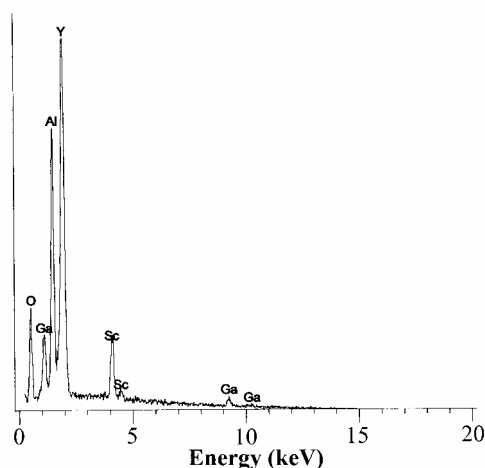


Fig. 5. Energy dispersive X-ray spectrum of $Y_3Sc_1Al_3Ga_1O_{12}$ ceramic sample

The appearance of scandium and gallium in the EDX spectra of both YSAGG samples is evident. Besides, Fig. 5 shows that intensity of Al line increases as compared with one in Fig. 4 and intensities of Sc and Ga lines decrease. These changes in the intensities of Al, Sc and Ga lines are in a good agreement with the chemical composition of investigated ceramic samples. Finally, EDX analyses of the synthesized $Y_3Sc_xAl_{5-x-y}Ga_yO_{12}$ samples showed that the content of metals in the separate crystallites corresponds to the nominal composition of starting materials, i.e. the syntheses yielded monophasic and homogeneous mixed-metal garnet samples.

IR spectra of calcined for 8 h at 1000 °C single-phase $Y_3Sc_xAl_{5-x-y}Ga_yO_{12}$ samples were obtained as well (Figs. 6 and 7).

A broad band at 3400 cm^{-1} which remains almost unchanged for different garnet samples can be assigned to the adsorbed water during the exposure of dried powder to air [8, 23]. The several intense bands in the range 900–450 cm^{-1} are characteristic of the metal-oxygen vibrations in the ceramic samples. According to Vaqueiro and Lopez-Quintela [8, 24] these bands are characteristic of YAG

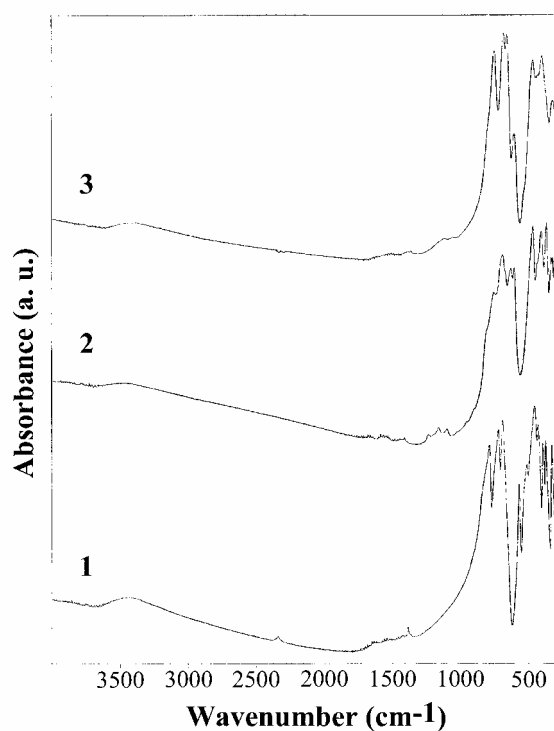


Fig. 6. IR spectra of different garnet samples: (1) $Y_3Al_5O_{12}$, (2) $Y_3Sc_2Al_1Ga_2O_{12}$ and (3) $Y_3Sc_1Al_3Ga_1O_{12}$

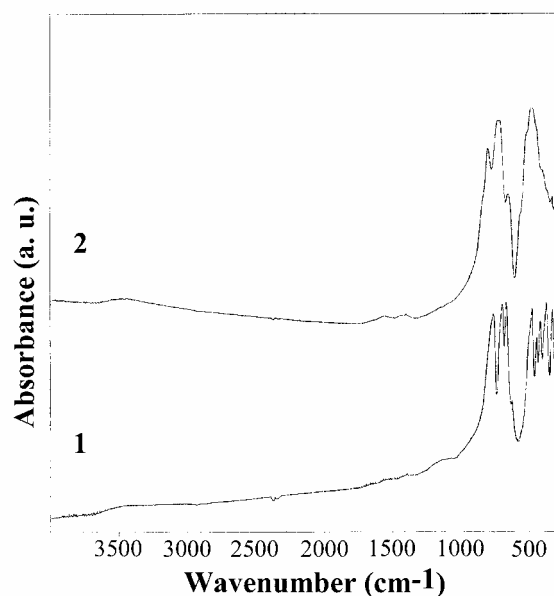


Fig. 7. IR spectra of different garnet samples: (1) $Y_3Sc_2Al_3O_{12}$ and (2) $Y_3Al_3Ga_2O_{12}$

structure and attributable to the stretching mode of the tetrahedral units in the garnet structure.

It is interesting to note that the observed characteristic stretching frequencies also are slightly shifted for different garnet compounds. Fig. 8 shows the dependence of the position of the first M–O peaks presented in all IR spectra of $Y_3Sc_xAl_{5-x-y}Ga_yO_{12}$ samples on the mean cationic radii at Al sites.

As seen from Fig. 8, wavenumber, consequently and frequency of the characteristic M–O vibrations in $Y_3Sc_xAl_{5-x-y}Ga_yO_{12}$ garnet samples decreases almost

linearly with increasing the mean cationic radius at Al sites. Such phenomenon was never observed previously in mixed-metal oxides, to our knowledge.

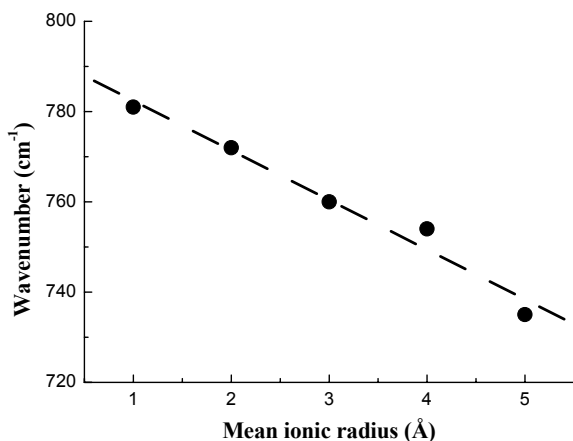


Fig. 8. The position of the first M–O peak as a function of mean cationic radius of the $Y_3Sc_xAl_{5-x-y}Ga_yO_{12}$ samples

The transmittance spectra of $Y_3Sc_xAl_{5-x-y}Ga_yO_{12}$ samples were measured at room temperature in the range of 200 – 1200 nm. Fig. 9 demonstrates the transmission spectrum of $Y_3Sc_1Al_3Ga_1O_{12}$ ceramic sample produced by sol-gel method.

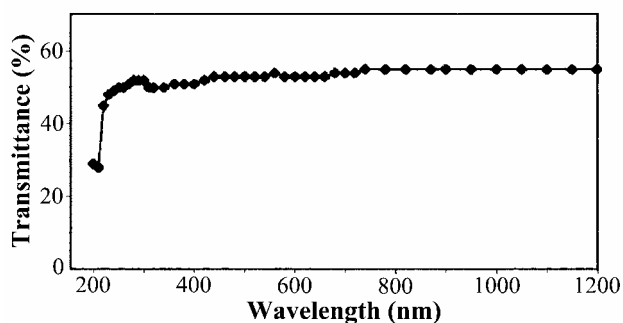


Fig. 9. The transmittance spectrum of $Y_3Sc_1Al_3Ga_1O_{12}$ garnet sample

As seen from Fig. 9, the absorption edge for the $Y_3Sc_1Al_3Ga_1O_{12}$ sample could be detected at ~210 nm. In UV range the garnet sample shows a significant decrease of transmission, which is required for optical materials [25 – 28]. In the higher wavelength region the transmission is almost constant, i.e. not wavelength dependent. Such garnet compound doped by rare-earth element would have an excellent optical quality [29].

Fig. 10 shows optical transmission spectrum of $Y_3Sc_2Al_3O_{12}$ ceramic sample.

As seen, the transmittance of $Y_3Sc_2Al_3O_{12}$ is slightly higher than that of $Y_3Sc_1Al_3Ga_1O_{12}$. Also, the absorption edge for the $Y_3Sc_2Al_3O_{12}$ is slightly shifted to the higher wavelength (~220 nm). Interesting fact is, that the recorded transmission spectrum for $Y_3Sc_2Al_1Ga_2O_{12}$ compound was found to be almost identical as for $Y_3Sc_2Al_3O_{12}$. It seems that intensity of transmittance and position of absorption edge correlate with the amount of scandium in the garnet. On the other hand, this can be attributed to the difference in the grain growth in the specimens [30]. However, the

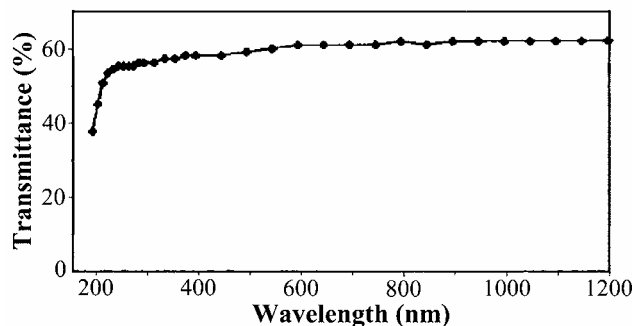


Fig. 10. The transmittance spectrum of $Y_3Sc_2Al_3O_{12}$ garnet sample

transmittance of $Y_3Al_5O_{12}$ and $Y_3Al_3Ga_2O_{12}$ samples was significantly lower to compare with those scandium-containing garnets. Moreover, the absorption edges for YAG and YAGG are located in low UV region (<200 nm). Therefore we can suggest that with increasing amount of scandium in the mixed-metal garnets the higher transmission and negligible shift in the absorption edge position are observed. These physical features, however, are independent on the amount of gallium in the investigated samples. Finally, high phase purity, good mechanical properties, broad transparent range of $Y_3Sc_xAl_{5-x-y}Ga_yO_{12}$ garnets make them an excellent candidates of host materials for advanced optical applications [31, 32].

CONCLUSIONS

Mixed-metal oxides $Y_3Sc_xAl_{5-x-y}Ga_yO_{12}$ ($0 \leq x, y \leq 5$) with different nominal composition were synthesized by aqueous sol-gel method. Sintering gels at 1000 °C produced fully crystalline single-phase compounds $Y_3Sc_1Al_3Ga_1O_{12}$, $Y_3Sc_2Al_1Ga_2O_{12}$, $Y_3Sc_2Al_3O_{12}$, and $Y_3Al_3Ga_2O_{12}$, with well pronounced garnet crystal structure. The XRD diffraction patterns showed negligible shift in the position of diffraction lines. The calculated d -spacing of a set of (420) planes, however, did not correlate with the mean cationic radii at Al sites for the single-phase $Y_3Sc_xAl_{5-x-y}Ga_yO_{12}$ samples. It was determined that the frequency of the characteristic M–O vibrations in $Y_3Sc_xAl_{5-x-y}Ga_yO_{12}$ garnet samples decreased almost linearly with increasing the mean cationic radius at Al sites. Such phenomenon was never observed previously in mixed-metal oxides, to our knowledge. The optical transmittance spectra showed that transmission and absorption edge position are slightly dependent on the amount of scandium in the mixed-metal garnets.

REFERENCES

1. Atwood, D. A., Yearwood, B. C. The Future of Aluminum Chemistry *J. Organomet. Chem.* 600 2000: pp. 186 – 197.
2. Wang, Y., Li, D. X., Thomson, W. J. The Influence of Steam on Mullite Formation from Sol-gel Precursors *J. Mater. Res.* 8 1993: pp. 195 – 205.
3. Kareiva, A., Harlan, C. J., MacQueen, D. B., Cook, R., Barron, A. R. Carboxylate-substituted Alumoxanes as Processable Precursors to Transition Metal-aluminum and Lanthanide-aluminum Mixed-metal Oxides: Atomic Scale Mixing Via a New Transmetalation Reaction *Chem. Mater.* 8 1996: pp. 2331 – 2340.

4. **Malinowski, M., Piramidowicz, R., Frukacz, Z., Chadeyron, G., Mahiou, R., Joubert, M. F.** Spectroscopy and Up-conversion Processes in $\text{YAlO}_3:\text{Ho}^{3+}$ Crystals *Opt. Mater.* 12 1999: pp. 409 – 423.
5. **Gulgun, M. A., Putlayev, V., Ruhle, M.** Effects of Yttrium Doping α -alumina: I. Microstructure and Microchemistry *J. Am. Ceram. Soc.* 82 1999: pp. 1849 – 1856.
6. **Isobe, T., Omori, M., Uchida, S., Sato, T., Hirai, T.** Consolidation of $\text{Al}_2\text{O}_3\text{-Y}_3\text{Al}_5\text{O}_{12}$ (YAG) Eutectic Powder Prepared from Induction-melted Solid and Strength at High Temperature *J. Europ. Ceram. Soc.* 22 2002: pp. 2621 – 2625.
7. **Harlan, C. J., Kareiva, A., MacQueen, D. B., Cook, R. Barron, A. R.** Yttrium-doped Alumoxanes: A *Chimie Douce* route to $\text{Y}_3\text{Al}_5\text{O}_{12}$ (YAG) and $\text{Y}_4\text{Al}_2\text{O}_9$ (YAM) *Adv. Mater.* 9 1997: pp. 68 – 71.
8. **Vaqueiro, P., Lopez-Quintela, M. A.** Synthesis of Yttrium Aluminium Garnet by the Citrate Gel Process *J. Mater. Chem.* 8 1998: pp. 161 – 163.
9. **Walker Jr., E. H., Owens, J. W., Etienne, M., Walker, D.** The Novel Low Temperature Synthesis of Nanocrystalline MgAl_2O_4 Spinel Using “Gel” Precursors *Mater. Res. Bull.* 37 2002: pp. 1041 – 1050.
10. **Veith, M., Mathur, S., Kareiva, A., Jilavi, M., Zimmer, M., Huch, V.** Low Temperature Synthesis of Nanocrystalline $\text{Y}_3\text{Al}_5\text{O}_{12}$ (YAG) and Ce-doped $\text{Y}_3\text{Al}_5\text{O}_{12}$ Via Different Sol-gel Methods *J. Mater. Chem.* 9 1999: pp. 3069 – 3079.
11. **Leleckaite, A., Jasaitis, D., Kareiva, A.** Sol-gel Synthesis of Holmium- and Neodymium-doped Yttrium Aluminium Garnet *Materials Science (Medžiagotyra)* 7 2001: pp. 225 – 229.
12. **Jasaitis, D., Mulioliene, I., Sivakov, V., Shen, H., Rapalaviciute, R., Mathur, S., Kareiva, A.** From Precursors to Ceramic Materials. 1. Sol-gel Chemistry Approach in the Preparation of Precursors for the Advanced Optical Materials *Materials Science (Medžiagotyra)* 8 2002: pp. 156 – 160.
13. **Mulioliene, I., Jasaitis, D., Kareiva, A., Blaschkowski, B., Glaser, J., Meyer, H.-J.** Sol-gel Synthesis and Characterization of Mixed-metal Garnet $\text{Y}_3\text{ScAl}_3\text{GaO}_{12}$ (YSAGG) *J. Mater. Sci. Lett.* 22 2003: pp. 349 – 351.
14. **Mulioliene, I., Mathur, S., Jasaitis, D., Shen, H., Sivakov, V., Rapalaviciute, R., Beganskiene, A., Kareiva, A.** Evidence of the Formation of Mixed-metal Garnets Via Sol-gel Synthesis *Opt. Mater.* 22 2003: pp. 241 – 250.
15. **Peleckis, G., Tonsuaadu, K., Baubonyte, T., Kareiva, A.** Sol-gel Chemistry Approach in the Preparation of Precursors for the Substituted Superconducting Oxides *J. Non-Cryst. Solids* 311 2002: pp. 250 – 258.
16. **Baranauskas, A., Jasaitis, D., Kareiva, A.** Characterization of Sol-gel Process in the Y-Ba-Cu-O Acetate-tartrate System Using IR Spectroscopy *Vibr. Spectrosc.* 28 2002: pp. 263 – 275.
17. **Roy, S., Wang, L., Sigmund, W., Aldinger, F.** Synthesis of YAG Phase by a Citrate-nitrate Combustion Technique *Mater. Lett.* 39 1999: pp. 138 – 141.
18. **Weber, J. K. R., Krishnan, S., Ansell, S., Hixson, A. D., Nordine, P. C.** Structure of Liquid $\text{Y}_3\text{Al}_5\text{O}_{12}$ (YAG) *Phys. Rev. Lett.* 84 2000: pp. 3622 – 3625.
19. **MacKenzie, K. J. D., Kemmitt, T.** Evolution of Crystalline Aluminate from Hybrid Gel-derived Precursors Studied by XRD and Multinuclear Solid-state MAS NMR. II. Yttrium-aluminium Garnet, $\text{Y}_3\text{Al}_5\text{O}_{12}$ *Thermochim. Acta* 325 1999: pp. 13 – 18.
20. **Kall, P.-O., Grins, J., Olsson, P.-O., Liddell, K., Korgul, P., Thompson, D. P.** Preparation and Crystal Structure of U-phase $\text{Ln}_3(\text{Si}_{3-x}\text{Al}_{3+x})\text{O}_{12+x}\text{N}_{2-x}$ ($x \approx 0.5$, Ln = La, Nd) *J. Mater. Chem.* 1 1991: pp. 239 – 244.
21. **Vyshatko, N. P., Kharton, V., Shaula, A. L., Naumovich, E. N., Marques, F. M. B.** Structural Characterization of Mixed Conducting Perovskites $\text{La}(\text{Ga},\text{M})\text{O}_{3-\delta}$ (M = Mn, Fe, Co, Ni) *Mater. Res. Bull.* 38 2003: pp. 185 – 193.
22. **West, A. R.** Basic Solid State Chemistry. Chichester: John Wiley and Sons, 1997.
23. **Liu, Y., Zhang, Z.-F., King, B., Halloran, J., Laine, R. M.** Synthesis of Yttrium Aluminium Garnet from Yttrium and Aluminium Isobutyrate Precursors *J. Am. Ceram. Soc.* 79 1996: pp. 385 – 394.
24. **Vaqueiro, P., Lopez-Quintela, M. A.** Influence of Complexing Agents and pH on Yttrium-iron Garnet Synthesized by the Sol-gel Method *Chem. Mater.* 9 1997: pp. 2836 – 2841.
25. **Zhang, S., Cheng, Z., Lu, J., Li, G., Lu, J., Shao, Z., Chen, H.** Studies on the Effective Nonlinear Coefficient of $\text{GdCa}_4\text{O}(\text{BO}_3)_3$ Crystal *J. Cryst. Growth* 205 1999: pp. 453 – 456.
26. **Lechna-Marczynska, M., Podbielska, H.** Influence of the Temperature of Preparation Process on Refractive Index of Sol-gel Matrices *Optica Applicata* 31 2001: pp. 257 – 261.
27. **Ulatowska, A., Kudrawiec, R., Podbielska, H., Bryja, L., Misiewicz, J.** Transmittance Examination in Sol-gel Derived Matrices for Optoelectronic Applications *Opt. Mater.* 17 2001: pp. 247 – 250.
28. **Jiwei, Z., Bo, S., Xi, Y., Liangying, Z.** Preparation and Spectral Properties of Nd_2O_3 -doped Silica-based Glasses Prepared by the Sol-gel Process *Ceram. Int.* 28 2002: pp. 737 – 740.
29. **Jun, D., Peizhen, D., Jun, X.** The Growth of Cr^{4+} , Yb^{3+} : Yttrium Aluminium Garnet (YAG) Crystal and its Absorption Spectra Properties *J. Cryst. Growth* 203 1999: pp. 163 – 167.
30. **Ikesue, A., Yoshida, K., Kamata, K.** Transparent Cr^{4+} -Doped YAG Ceramics for Tunable Lasers *J. Am. Ceram. Soc.* 79 1996: pp. 507 – 509.
31. **Vega-Duran, J. T., Barbosa-Garcia, O., Diaz-Torres, L. A., Meneses-Nava, M. A.** Effects of Energy Back Transfer on the Luminescence of Yb and Er ions in YAG *Appl. Phys. Lett.* 76 2000: pp. 2032 – 2034.
32. **Gaume, R., Viana, B., Derouet, J., Vivien, D.** Spectroscopic Properties of Yb-doped Scandium Based Compounds $\text{Yb}:\text{CaSc}_2\text{O}_4$, $\text{Yb}:\text{SrSc}_2\text{O}_4$ and $\text{Yb}:\text{Sc}_2\text{SiO}_5$ *Opt. Mater.* 22 2003: pp. 107 – 115.